ELEKTROTEHNIŠKI VESTNIK 87(5): 243-250, 2020
ORIGINAL SCIENTIFIC PAPER

Impact of reactive grid support strategies on power quality in photovoltaic systems

Walid Rahmouni [1] , Ghalem Bachir [1], Michel Aillerie[2]

[1]*Laboratoire de Développement Durable de l'Energie Electrique (LDDEE), Université des Sciences et de la Technologie d'Oran*
[2]*Laboratoire Matériaux Optiques, Photonique et Systèmes (LMOPS), Université de Lorraine, Metz, France*
E-mail: Walid.rahmouni@univ-usto.dz

Abstract. Despite the advances in renewable technologies, power-quality implications remain some of the most challenging aspects when it comes to grid integration. Grid codes and procedures regarding harmonic injection only consider the rated output power under standard test conditions. However, with reactive grid-support strategies gaining interest, the power-quality limits may be exceeded. The paper offers a harmonic investigation of grid-tied photovoltaic systems under the reactive-grid support scenarios. The harmonic spectrum is investigated relative to the fundamental current, and voltage and total demand current. A 100 kW grid-connected photovoltaic system is simulated on Matlab-Simulink through different study cases. The impact on the switching harmonics is found to be linear. On the other hand, the lower-order harmonics behave differently and either improve or worsen the power quality depending on the reactive operating point. Different irradiance values are also investigated and seem to have no negative effect considering the applicable IEEE standards. The work highlights the importance of the power-quality assessement in photovoltaic systems with dispatchable reactive-power capabilities.

Keywords: Photovoltaic system, Total harmonic distortion, Reactive-power control, Grid-connected inverter, Power quality.

Vpliv jalove energije na kakovost električne energije v fotovoltaičnih sistemih

Kljub napredku na področju obnovljivih tehnologij ima kakovost električne energije velik pomen pri vključevanju generatorjev v električno omrežje. Pravila delovanja električnega omrežja in postopki v zvezi z vnosom višjeharmonskih komponent upoštevajo le nazivno izhodno moč pri standardnih preizkusnih pogojih (STC). V članku predstavljamo harmonsko analizo omrežnih fotonapetostnih sistemov pri različnih vplivih jalove energije. Harmonski spekter smo analizirali glede na osnovni tok, napetost in skupni tok porabe. Fotovoltaični sistem moči 100 kW smo simulirali v programskem okolju Matlab-Simulink na različnih študijskih primerih. Ugotovili smo, da je vpliv na preklopne harmonike linearen. Nižjeharmonske komponente lahko ali izboljšajo ali poslabšajo kakovost električne energije. Raziskali smo tudi različne vplive osvetlitve, ki nimajo negativnih vplivov po standardu IEEE 519-2014. V članku je predstavljen pomen ocene kakovosti električne energije v fotovoltaičnih sistemih z zmožnostjo oddaje jalove energije.

1 INTRODUCTION

Renewable energies play a crucial role in electric power generation, and are becoming essential these days due to the shortage and environmental impacts of conventional fuels [1]. Among the various possible sources, the solar energy is dominant because of its abundant availability [2].

The last decade has witnessed the fast-spread applications of the photovoltaic (PV) power all around the world. It is one of the most mature renewable generation technologies [3]. Moreover, the quickly decreasing prices of the PV technology has boosted its installation globally [4]. According to the International Renewable Energy Agency (IRENA), the cumulative installed capacity of PV sources worldwide was around 385 GW in 2017 and 480 GW in 2018 [5]. It is expected to reach 2.8 TW by 2030 and 8.5 TW by 2050, 60% of which will be of the utility scale [6].

However, the large-scale integration of PV systems creates additional technical challenges [7]. The inverter-based interfaces give rise to the current and voltage harmonics, which may damage the power system devices and negatively impact the efficiency and reliability of the network [8]. The harmonic orders may vary from 2 to 100 and even more. Most standards

Received 23 August 2020
Accepted 10 November 2020

consider 50 orders, yet, harmonic studies usually analyze the first 25 orders due to their significant magnitudes compared to the higher orders [9]. The low-order harmonics, mainly the 5th, 7th and a series of odd harmonics, are found to be caused by the DC-link voltage ripple [10]. The Switching harmonics depend on the inverter switching frequency. In [11], these harmonics have been found around the 38th order. The switching harmonics are more difficult to eliminate and may require a suitable control design [12].

The fluctuating solar irradiance strongly inter-relationed with the power-quality index. The solar-irradiance-dependent level of harmonic distortion has been investigated by several researchers. Individual harmonic current spectrum and current THD values are much higher in low solar-irradiance conditions than those in high solar-irradiance conditions [7], [8]. The harmonic current spectrum also depends on the PV system output power, which is proportional to the solar irradiance. However, solar inverters cannot always work under rated conditions [13].

With the increasing share of the PV energy in the electric power grid, the demand of producing the reactive power becomes more and more justified [14]. Several reactive-power compensation strategies have been proposed and investigated in order to make the best use of the inverter potential under low solar irradiance scenarios. Even though the available active power is an intermittent function of the solar irradiance available, the reactive-power generated can be controlled by the inverter, in either a reactive-power, power-factor or voltage-control mode [15]. Various techniques can be utilized for this purpose [16]. Traditionally, this is done by employing a control scheme in the inverter control circuit [17].

The operating points of the PV systems are dependent on the control strategy adopted. However, utility standards and manufacturers data sheets are only concerned with the full-load states [10], [13]. Therefore, reviewing the power-quality implications of the reactive-grid support strategies is vital. Considering the huge amount of economic losses and technical problems involved, harmonic levels across the inverter reactive capability should be considered in the dispatch.

The paper investigates the harmonic impact of the reactive-control strategy in PV inverters. It is organized as follows. Section 2 describes the studied PV system. Section 3 focuses on the concept of the harmonic and its implications. Section 4 presents the simulation studies of a 100 Kw grid-connected system on Simulink Matlab. Results of the harmonic spectrum are presented. The THD_i, THD_v and TDD are calculated using the Fast Fourier Transform. Finally, Section 5 draws conclusions.

2 SYSTEM DESCRIPTION

The modeled conversion chain is presented in Fig. 1. It consists of a PV array, DC/DC (Direct Current) converter with an MPPT control, DC/AC inverter with a PWM (Pulse Width Modulation) control, passive filter and grid or load [18].

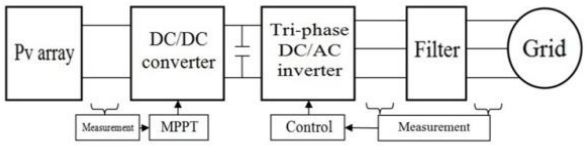

Figure 1. Block diagram of a two-stage PV system.

2.1 PV array

The PV array is the main subsystem responsible for the energy conversion from the solar irradiance to the DC output power [15]. It is usually composed of several PV panels (or modules) in series and parallel connections [19].

Fig. 2 shows the equivalent electric circuit of a solar PV cell. The model consists of a current source (I_{PH}) representing the light-generated current in the cell, parallel diode, series resistance (R_s) and shunt resistance (R_{sh}). The shunt resistance represents the junction leakage-current part.

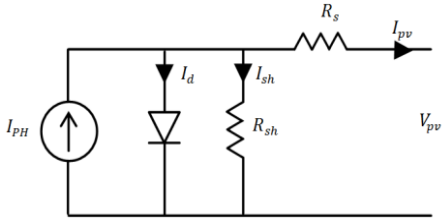

Figure 2. Equivalent model of a PV cell.

The I-V characteristic expression of the PV cells corresponding to the general equivalent circuit is shown in Eq. (1) [20]:

$$I_{pv} = I_{PH} - I_{sat}\left[\exp\left(q\,(V_{pv} + \frac{(I_{pv}\,R_s)}{AKT})\right) - 1\right] - (V_{pv} + \frac{(I_{pv}\,R_s)}{R_{sh}}) \quad (1)$$

Where:
T - cell temperature in Kelvin (K),
I_{sat} - reverse saturation current (A),
q - electron charge ($1.6022*10^{-19}$ C),
I_{pv} - solar cell output current (A),
V_{pv}- solar cell output voltage (V),
A - ideality factor and
K - Boltzman constant ($1.38*10^{-23}$ J/k).

Another particular phenomenon of the PV generation is the power-generation bell curve during the day. As the sun rises, PV panels can produce an increasing amount of electricity. As the sun sets, the power production decreases [15].

The solar irradiance directly affects the light-generated current (I_{PH}). The irradiance model for a clear sky (S_{simple_sky}) is characterized by the parameters of the peak solar irradiance (S_{max}), sunrise time (t_{rise}) and sunset time (t_{set}) as follows [21]:

$$S_{simple\ sky} = \begin{cases} 0\ , t \le t_{rise} \\ S_{max} \sin\left(\frac{\pi(t-t_{rise})}{(t_{set}-t_{rise})}\right),\ t_{set} < t < t_{rise} \\ 0\ , t \ge t_{set} \end{cases} \quad (2)$$

2.2 DC/DC Boost converter

The boost converter is used for stepping up the input voltage. It consists of a capacitor, inductor and diode as shown in Fig. 3. The relationship between the input-output voltage of the Boost Converter is given in Eq. (3) [22]

$$V_o = V_i/(1-\alpha) \quad (3)$$

where V_i is the input voltage, V_o is the output voltage and α is the duty cycle.

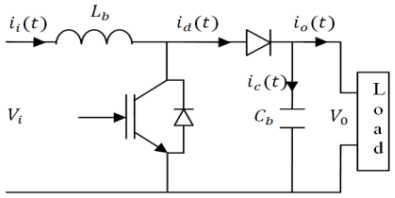

Figure 3. DC-DC boost-converter circuit.

2.3 MPPT control

The maximum power output of a PV array is a unique operating point obtained from the non-linear PV characteristics [23]. The maximum power point tracking (MPPT) is an essential control algorithm to detect the maximum input power corresponding to fluctuations on the source voltage and current [24].

One of the simplest and most commonly used MPPT methods is the Perturb and Observe (P&O) [25]. It works on the principle that if the PV module operating voltage changes and the power increases, the control system moves the operating point in that direction. In the opposite case, the operating point is moved in the opposite direction. The flowchart of this technique is shown in Fig. 4 [1].

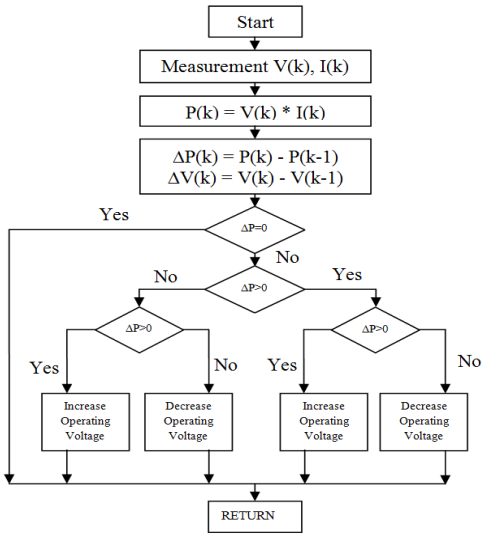

Figure 4. Flowchart of the P&O algorithm.

2.4 DC/AC inverter

The inverter is used to deliver the energy from the PV-array side to the utility grid [26]. It converts the generated DC power into an AC power according to a chosen control scheme and converter topology [15]. The inverter output is controlled by a closed-loop control system in order to react to changes observed at its terminals [27]. Two separate control infrastructures are used. One controls the DC bus voltage and the other the active and reactive power delivered to the grid [24], [26]. The switching pulses are generated by comparing the sinusoidal reference waveform to a triangular waveform (PWM) [18].

The Proportional Integral (PI) control method depicted in Fig. 5 is normally used for the grid-connected inverter [9]. The controller transforms the grid phase voltages (V_a V_b, V_c), and currents (I_a I_b, I_c) from the stationary reference frame into their DC components, (V_d, V_q) and (I_d, I_q), in the synchronous rotating reference frame as described in Eq. (4) [28].

$$\begin{bmatrix} d \\ q \\ 0 \end{bmatrix} = \left(\frac{2}{3}\right) \begin{bmatrix} \cos(\theta) & \cos\left(\theta - \frac{2\pi}{3}\right) & \cos\left(\theta + \frac{2\pi}{3}\right) \\ -\sin(\theta) & -\sin\left(\theta - \frac{2\pi}{3}\right) & -\sin\left(\theta + \frac{2\pi}{3}\right) \\ \frac{1}{2} & \frac{1}{2} & \frac{1}{2} \end{bmatrix} \begin{bmatrix} a \\ b \\ c \end{bmatrix} \quad (4)$$

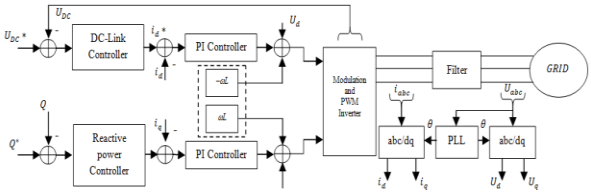

Figure 5. PI controller model for grid-tied inverter.

The PV inverter performance is limited by the rated power as well as by the maximum power provided by the PV source [29]. It can contribute a significant amount of the reactive power during normal and even fault operating states. Traditionally, this is done by employing a control scheme in the inverter control circuit [17] capable of operating at any combination of the active (P) and reactive (Q) power within a range delimited by its capability curve. These diagrams provided by the manufacturer depict the performance of an individual inverter based on the capacity limits of the active and reactive power [30]. An example of the inverter power-quality diagram is illustrated in Fig. 6 [29].

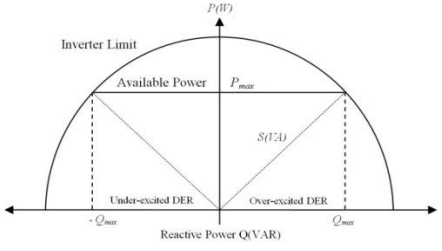

Figure 6. Example of an inverter capability curve.

3 HARMONIC DISTORTION

A sinusoidal voltage is a conceptual quantity produced by an ideal AC generator, built with a finely-distributed stator and field windings, operating in a uniform magnetic field which does not exist in practice [9]. Any distortion in the sinusoidal nature of the AC wave deviates the power quality which is termed as harmonic [2]. Harmonics are sinusoidal components with frequencies that are integer multiples of the fundamental supply frequency [7].

The commonly used indicator to reflect the distortion levels is the Total Harmonic Distortion (THD) which is the ratio of the rms magnitude of the harmonics (excluding the fundamental) to the fundamental rms value. THD can be calculated for the voltage and current as follows [13].

$$\mathrm{THD_i} = \left(\sqrt{\sum_{h>1}^{h_{max}} \mathrm{I_h}^2}\right)/\mathrm{I_F} \quad (5)$$

$$\mathrm{THD_v} = \left(\sqrt{\sum_{h>1}^{h_{max}} \mathrm{V_h}^2}\right)/\mathrm{V_F} \quad (6)$$

whrere I_F is the rms fundamental current, I_h is the rms value of the current at the h^{th} harmonics, V_F is the rms fundamental current and V_h is the rms value of the voltage at the h^{th} harmonics.

The Total Demand Distortion (TDD) is very similar to the THD, except for the denominator. In the TDD, the harmonics are expressed as a percentage of I_L (maximum demand load current) and THD expresses the harmonic content as a percentage of I_F (fundamental current) [31]. Its expression is shown in Eq. (7).

$$\mathrm{TDD} = \left(\sqrt{\sum_{h>1}^{h_{max}} \mathrm{I_h}^2}\right)/\mathrm{I_L} \quad (7)$$

Usually, THD is measured first and then a comparison is made to the limits. If there is a problem, TDD is calculated. It is rarely needed to convert to TDD, which is why the THD concept is much better known [29]. Nevertheless, the IEEE 519 standard makes a clear distinction between the THD_i and TDD concept. It limits the voltage THD at the point of common coupling (PCC) and TDD in terms of the maximum short-circuit current at PCC (I_{sc}) as shown in Tables. 1 and. 2, respectively [32].

Excessive harmonic voltage and current levels induce extra losses, like core losses in transformers and generators, and increase transmission losses in conductors resulting in them overheating, also affecting the power-equipment lifecycles and potentially also mal-operation of protective devices [2], [13].

Table 1. Voltage distortion limits.

Bus voltage V at PCC	Individual harmonic (%)	Total harmonic distortion THD (%)
$V \leq 1.0kV$	5.0	8.0
$1kV < V \leq 69kV$	3.0	5.0
$69kV < V \leq 161kV$	1.5	2.5
$161kV \leq V$	1.0	1.5

Table 2. Current-distortion limits for systems rated 120V through 69 kV.

Maximum harmonic current distortion in percent of I_L						
Individual harmonic order (odd harmonics)						
I_{sc}/I_L	$3 \leq V < 11$	$11 \leq V < 17$	$17 \leq V < 23$	$23 \leq V < 35$	$35 \leq V \leq 50$	TDD
<20	4.0	2.0	1.5	0.6	0.3	5.0
20<50	7.0	3.5	2.5	1.0	0.5	8.
50<100	10.0	4.5	4.0	1.5	0.7	12.0
100<1000	12.0	5.5	5.0	2.0	1.0	15.0
>1000	15.0	7.0	6.0	2.5	1.4	20.0

4 RESULTS AND DISCUSSION

To examine the effects of the reactive-grid support strategy on the power quality, simulations are performed in the MATLAB/Simulink environment. The harmonic pollution is assessed using the Total Current and Voltage Harmonic Distortion ($\mathrm{THD_i}$ and $\mathrm{THD_v}$) and Total Demand Distortion (TDD).

The studied system is a 100 kW grid-connected PV system shown in Fig. 7. It consists of a PV array connected to a DC-DC boost converter and interfaced with the grid through a three-phase inverter, LCL filter and three-phase transformer. A 100 kW load is connected on an AC bus. The system parameters are given in Table 3. The inverter reactive-power capability ranges from -0.5 p.u to +0.5 p.u.

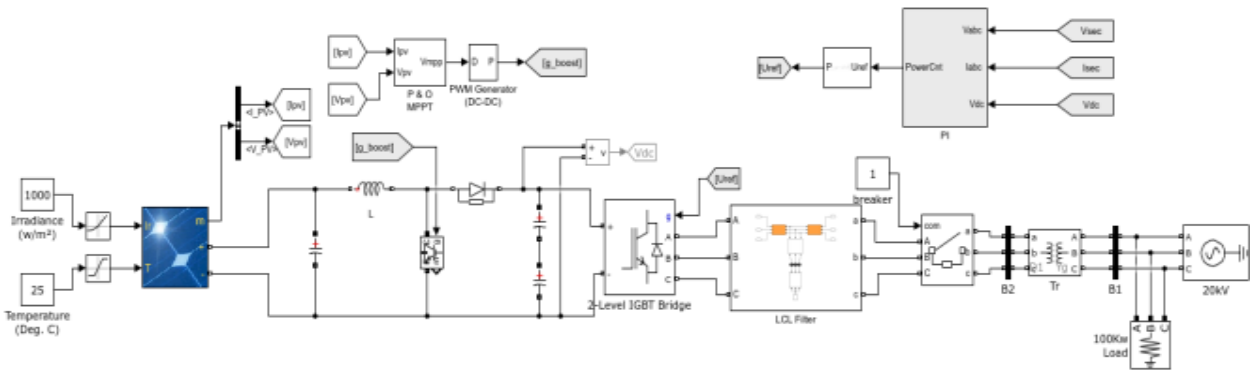

Figure 7. Test system in the Matlab-Simulink environment.

Table 3. Specifications of the studied system.

Pv array	
Open circuit voltage (V_{oc})	64.6 [V]
Optimum operating voltage (V_{mpp})	54.7 [V]
Short circuit current (I_{oc})	6.14 [A]
Optimum operating current (I_{Mpp})	5.76 [A]
Maximum power (P_{mpp})	315.072 [W]
Number of cells per module (N_s)	96
Series-connected modules per string (N_{ss})	5
Parallel strings (N_{pp})	64
Boost converter	
Inductance (L_b)	0.173 [mH]
Input capacitor (C_b)	1300 [µF]
Output capacitor (C_{dc})	24 [mF]
LCL filter	
Input inductance (L_i)	0.427 [mH]
Filter Capacitor (C_f)	2350 [µF]
Damping resistor (R_d)	0.269 [Ω]
Grid-side inductance (L_g)	0.238 [mH]
Simulation	
Grid frequency (f_c)	50 [Hz]
Switching frequency (f_n)	33**fn* [KHz]
Simulation time-step (t)	1e-6 [s]

The PV systems are generally utilized in places with high solar irradiance levels. However, their operating point will change across the day or due to the weather conditions. The THD_i calculations reported in Fig. 8 for different irradiance values show a higher current harmonic distortion for lower irradiance levels. The reactive power generated or absorbed noticeably improves the power quality. This phenomenon is more pronounced in the low-irradiance levels (250w/m²), with THD close to 6.5% in normal operating states. It gets to 3.5% for 0.5 p.u of the reactive compensation and 2.5% for 0.5p.u of the reactive absorption.

A detailed irradiance-dependant harmonic spectrum is presented in Fig. 9. It considers the odd harmonics up to the 50th order, as per the IEEE 519-2014 standard. The results are in agreement with those reported in the literature. In general, the power quality in a PV system is a function of the solar irradiance. A higher current distortion is noticed for lower irradiance levels. However, according to most standards, only THD_v and TDD are limited. The two indices are shown in Figs. 10 and 11, respectively, along with the most relevant harmonic orders. Irradiance has little to no impact on both indices. The conclusion is that the THD_i values are mostly caused by a lower fundamental current accordingly with Eq. (5).

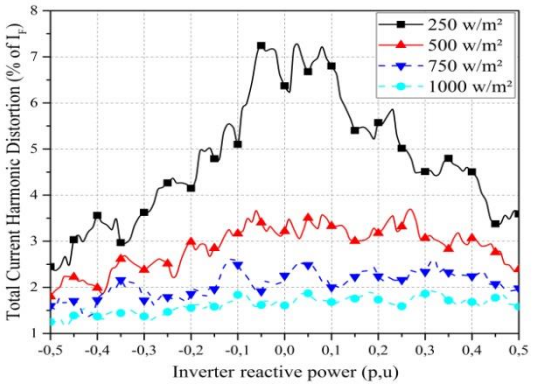

Figure 8. Current THD through reactive variations at different irradiance values.

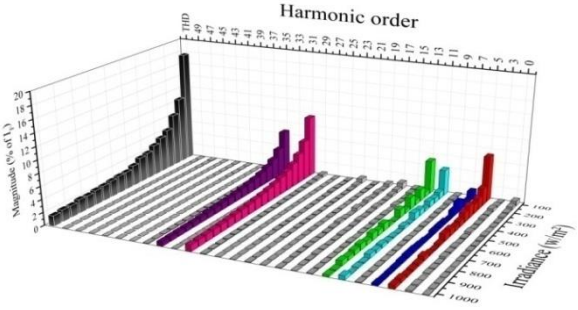

Figure 9. Irradiance impact on the current harmonic spectrum.

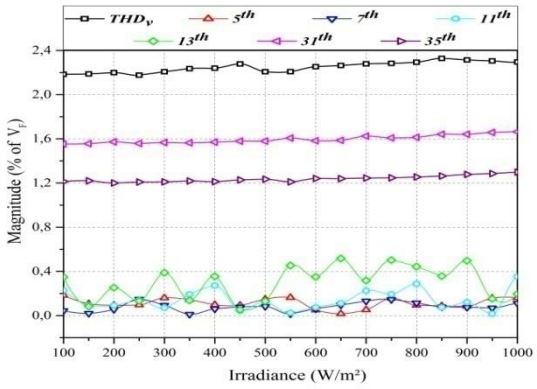

Figure 10. Voltage harmonic spectrum and THDv at irradiance variations.

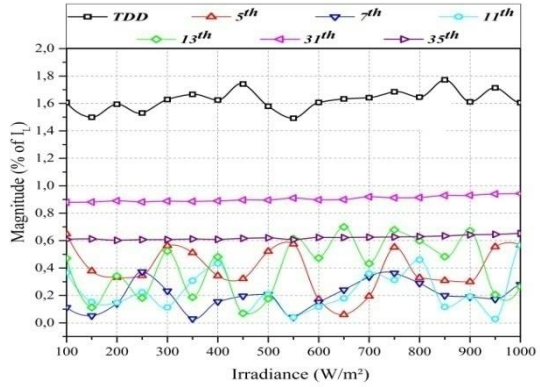

Figure 11. Current harmonic spectrum in % of IL and TDD at irradiance variations.

Some of the major sources of distortion are the switching pulses responsible for the high-order harmonics. Their behavior is examined through a complete current harmonic spectrum shown in Fig. 12. The predominant 31th and 35th orders are directly linked with the switching frequency. Figs. 13 and 14 render the voltage components of the switching harmonics with respect to the fundamental (V_F) and their currents with respect to the total demand current (I_L), respectively.

The three indices have a tendency to increase with the increase in the reactive power. The total distortion is greatly affected by the high components of the switching harmonics which exceed the standard admissible limits in this case. Both the voltage and current components seem to have a linear relationship with the reactive power injected by the inverter. Reactive absorption brings the switching harmonic current magnitudes closer to their admissible values (0.6% and 0.3% for the 31th and 35th orders, respectively). It is possible that the inductive nature of the reactive power acts like an additional "L-filter" which lowers the harmonics.

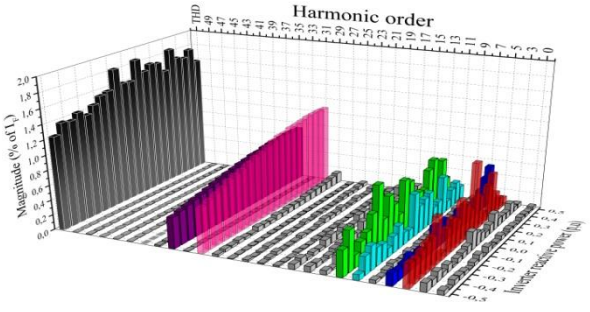

Figure 12. Current harmonic spectrum with respect to the inverter reactive power.

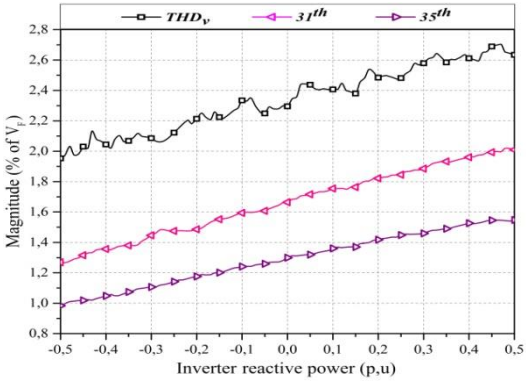

Figure 13. Voltage harmonic spectrum and THDv with respect to the inverter reactive power.

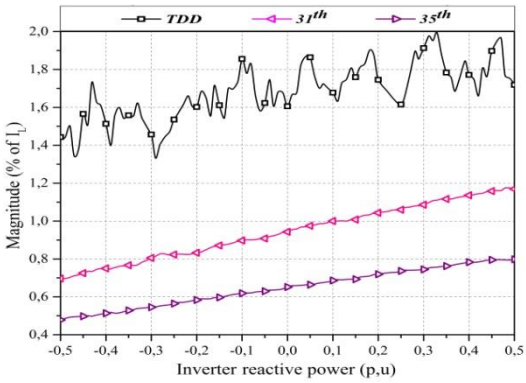

Figure 14. Current harmonic spectrum in % of IL and TDD with respect to the inverter reactive power

In order to minimise the switching harmonics impact on the power quality, a higher switching frequency is used (f_c=100 f_n). This moves the switching harmonics to the 98th and 102nd orders which impacts are negligible (with magnitudes of 0.25% and 0.24%, respectively, in normal operating states). The current harmonic spectra of the system are given in Fig. 15 showing a dominance of the 5th, 7th, 11th and 13th harmonics. Figs. 16 and 17 render their voltage components with respect to the fundamental (V_F) and their currents with respect to the total demand current (I_L), respectively.

The voltage components closely mimic the current components. They both show variations in the distortion levels for different reactive values. The higher peaks can be observed at 0.05 p.u and 0.3 p.u while minima are observed at -0.5 p.u, -0.1 p.u , 0.15 p.u and 0.3p.u. This behavior is found with the odd-order harmonics, especially the 13th which has the highest value.

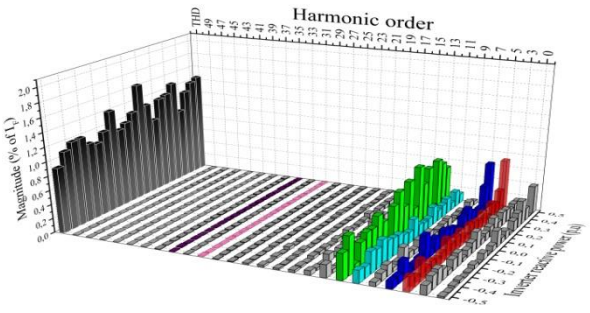

Figure 15. Current harmonic spectrum at reactive-power variations.

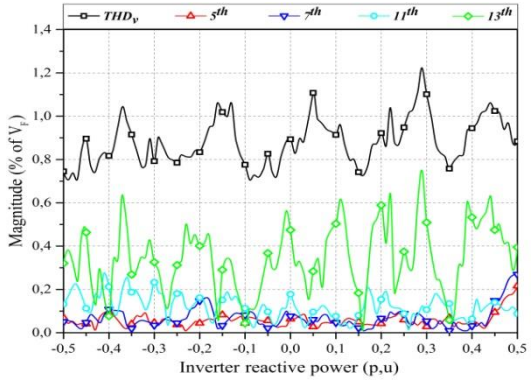

Figure 16. Voltage harmonic spectrum and THDv at reactive-power variations.

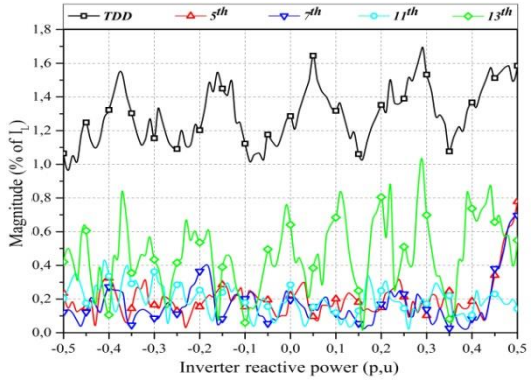

Figure 17. Current harmonic spectrum in % of IL and TDD at reactive-power variations.

5 Conclusion

The development of PV systems has led to an increasing usage of reactive-grid support strategies for the voltage and power-factor management. However, to the best of the author's knowledge, there has been no study related to the impact of these strategies on the power quality and harmonic generation. In the work, the reactive-grid support power quality implications are investigated. The main focus is to explore the behavior of the harmonic indices (THD_i, THD_v and TDD) through simulations of a PV test system on Matlab/Simulink.

Throughout the explored cases, reactive control is shown to have a great impact on the power quality. Firstly, a linear relationship with the switching harmonics is noticed. The harmonic distortion has a tendency to decrease with the reactive absorption in a system with a high content of the switching harmonics. The reactive injection, on the other hand, has an aggravating effect.

Moreover, the odd-order harmonics do not follow a clear identifiable pattern. Nonetheless, peaks in the harmonic distortion can be observed at different operating points. The reactive power leads to a 23% increase or reduction in the current and voltage harmonic distortions depending on its value. This phenomenon can cause a violation of the standards limits if not considered.

The harmonic spectrum values are found to be independent of the irradiance. Reactive support has the same effect regardless of the irradiance. The exception would be while considering THD_i which increases with lower irradiance values due to the lower fundamental current. This phenomenon should not be an issue and is not a risk factor for the equipements. Thus it is not considered in standard limitations.

In conclusion, this work highlights the importance of harmonic consideration when it comes to the reactive-power management in grid-connected PV systems. The reactive-power control can either reduce or worsen the harmonic distortion. This needs to be taken into consideration in the reactive-power dispatch. It is even more important for the systems operating close to the limits in normal operating states.

Furthermore, investigating real-time optimization techniques might provide a powerful tool in determining an optimal operating point with the lowest power-quality implications while supporting the grid with the reactive power. It would be a powerful tool for harmonic-reduction purposes in highly distorted systems.

References

[1] H. Rezk and A. M. Eltamaly, “A comprehensive comparison of different MPPT techniques for photovoltaic systems,” Sol. energy, vol. 112, pp. 1–11, 2015.

[2] S. Parthasarathy and N. V Anandkumar, “Effect of Fluctuating Solar Irradiance on the Quality of Power Generated by Solar Photovoltaic System,” Int. J. Adv. Eng. Res. Technol., vol. 5, no. 9, pp. 657–664, 2017.

[3] J. Ma, D.-W. Zhao, M.-H. Qian, L.-Z. Zhu, and H. Geng, “Modelling and validating photovoltaic power inverter model for power system stability analysis,” J. Eng., vol. 2017, no. 13, pp. 1605–1609, 2017.

[4] M. Tomi, P. Blaž, and G. Andrej, “Enhancing the economic benefit of fair PV curtailment with an improved remuneration mechanismNo Title,” Elektroteh. Vestnik/Electrotechnical Rev., vol. 82, no. 5, pp. 287–296, 2015.

[5] IRENA, “Renewable capacity statistics 2019,” Abu Dhabi, 2019. [Online]. Available: https://www.irena.org/publications.

[6] IRENA, “Future of Solar Photovoltaic: Deployment, investment, technology, grid integration and socio-economicaspects (A Global Energy Transformation: paper),” Abu Dhabi, 2019. [Online]. Available: https://www.irena.org/publications.

[7] A. Vinayagam, A. Aziz, P. M. Balasubramaniyam, J. Chandran, V. Veerasamy, and A. Gargoom, “Harmonics assessment and

mitigation in a photovoltaic integrated network," Sustain. Energy, Grids Networks, vol. 20, p. 100264, 2019.

[8] I. C. Barutcu, E. Karatepe, and M. Boztepe, "Impact of harmonic limits on PV penetration levels in unbalanced distribution networks considering load and irradiance uncertainty," Int. J. Electr. Power Energy Syst., vol. 118, p. 105780, 2020.

[9] A. Kalair, N. Abas, A. R. Kalair, Z. Saleem, and N. Khan, "Review of harmonic analysis, modeling and mitigation techniques," Renew. Sustain. Energy Rev., vol. 78, pp. 1152–1187, 2017.

[10] Y. Du, D. D.-C. Lu, G. James, and D. J. Cornforth, "Modeling and analysis of current harmonic distortion from grid connected PV inverters under different operating conditions," Sol. Energy, vol. 94, pp. 182–194, 2013.

[11] K. Yang, M. H. J. Bollen, E. O. A. Larsson, and M. Wahlberg, "Measurements of harmonic emission versus active power from wind turbines," Electr. Power Syst. Res., vol. 108, pp. 304–314, 2014, doi: 10.1016/j.epsr.2013.11.025.

[12] A. M. Abu-Mahfouz, O. A. Ajeigbe, S. P. Chowdhury, and T. O. Olwal, "Harmonic Control Strategies of Utility-ScalePhotovoltaic Inverters," Int. J. Renew. energy Res., vol. 8, no. 3, 2018.

[13] L. Xiong, M. Nour, and E. Radwan, "Harmonic Analysis of Photovoltaic Generation in Distribution Network and Design of Adaptive Filter," Int. J. Comput. Digit. Syst., vol. 9, 2020.

[14] B. Kristijan and T. Marko, "Energy and Economic Yield of Photovoltaic Systems: Reactive-Power Impact," Elektroteh. Vestnik/Electrotechnical Rev., vol. 81, pp. 9–14, 2014.

[15] L. Kunjumuhammed, S. Kuenzel, and B. Pal, Simulation of Power System with Renewables. Elsevier Inc, 2020.

[16] N. Gira and A. K. Dahiya, "Solar PV-BES in distribution system with novel technique for DC voltage regulation," Eng. Sci. Technol. an Int. J., 2020, doi: 10.1016/j.jestch.2020.01.004.

[17] M. N. I. Sarkar, L. G. Meegahapola, and M. Datta, "Reactive power management in renewable rich power grids: A review of grid-codes, renewable generators, support devices, control strategies and optimization Algorithms," IEEE Access, 2018, doi: 10.1109/ACCESS.2018.2838563.

[18] A. Azizi et al., "Impact of the aging of a photovoltaic module on the performance of a grid-connected system," Sol. energy, vol. 174, pp. 445–454, 2018, doi: 10.1016/j.solener.2018.09.022.

[19] R. Tang, "Large-scale photovoltaic system on green ship and its MPPT controlling," Sol. Energy, vol. 157, pp. 614–628, 2017, doi: 10.1016/j.solener.2017.08.058.

[20] W. Shinong, M. Qianlong, X. Jie, G. Yuan, and L. Shilin, "An improved mathematical model of photovoltaic cells based on datasheet information," Sol. Energy, vol. 199, pp. 437–446, 2020, doi: 10.1016/j.solener.2020.02.046.

[21] T. Sung, S. Yoon, and K. Kim, "A Mathematical Model of Hourly Solar Radiation in Varying Weather Conditions for a Dynamic Simulation of the Solar Organic Rankine Cycle," Energies, vol. 8, pp. 7058–7069, 2015, doi: 10.3390/en8077058.

[22] S. Dorji, D. Wangchuk, T. Choden, and T. Tshewang, "Maximum Power Point Tracking of solar photovoltaic cell using Perturb & Observe and fuzzy logic controller algorithm for boost converter and quadratic boost converter," Mater. Today Proc., 2020, doi: 10.1016/j.matpr.2020.02.144.

[23] J. P. Ram, D. S. Pillai, A. M. Y. M. Ghias, and N. Rajasekar, "Performance enhancement of solar PV systems applying P&O assisted Flower Pollination Algorithm (FPA)," Sol. Energy, vol. 199, pp. 214–229, 2020, doi: 10.1016/j.solener.2020.02.019.

[24] E. Kabalcı, "Review on novel single-phase grid-connected solar inverters: Circuits and control methods," Sol. Energy, vol. 198, pp. 247–274, 2020, doi: 10.1016/j.solener.2020.01.063.

[25] M. K. Mishra and V. N. Lal, "An improved methodology for reactive power management in grid integrated solar PV system with maximum power point condition," Sol. Energy, vol. 199, pp. 230–245, 2020, doi: 10.1016/j.solener.2020.02.001.

[26] A. I. M. Ali, M. A. Sayed, and E. E. M. Mohamed, "Modified efficient perturb and observe maximum power point tracking technique for grid-tied PV system," Electr. Power Energy Syst., vol. 99, pp. 192–202, 2018, doi: 10.1016/j.ijepes.2017.12.029.

[27] D. Fetzer et al., "Modelling of small-scale photovoltaic systems with active and reactive power control for dynamic studies," in the 6th Solar Integration Workshop proceedings, 2016.

[28] A. A. S. Mohamed, H. Metwally, A. El-Sayed, and S. I. Selem, "Predictive neural network based adaptive controller for grid-connected PV systems supplying pulse-load," Sol. Energy, vol. 193, pp. 139–147, 2019, doi: 10.1016/j.solener.2019.09.018.

[29] R. Darbali-Zamora, A. Summers, J. Hernandez-Alvidrez, J. E. Quiroz, J. Johnson, and E. I. Ortiz-Rivera, "Exponential Phase-Locked Loop Photovoltaic Model for PHIL Applications," 2018, pp. 1–6, doi: 10.1109/ANDESCON.2018.8564592.

[30] E. H. Enrique, "Use of capability curves for the analysis of reactive power compensation in solar farms," in 2017 IEEE/IAS 53rd Industrial and Commercial Power Systems Technical Conference (I&CPS), 2017, pp. 1–6.

[31] A. Lucas, F. Bonavitacola, E. Kotsakis, and G. Fulli, "Grid harmonic impact of multiple electric vehicle fast charging," Electr. Power Syst. Res., vol. 127, pp. 13–21, 2015, doi: 10.1016/j.epsr.2015.05.012.

[32] IEEE Power and Energy Society, "IEEE Recommended Practice and Requirements for Harmonic Control in Electric Power Systems," IEEE Std. 519-2014, 2014.

Walid RAHMOUNI received the Master degree in electrical engineering in 2016 from the University of science and technology of Oran Mohamed Boudiaf (USTO-MB), Algeria, where he is currently preparing a Doctorate thesis in Power system engineering with the Laboratory of sustainable developpement of the electric energy (LDDEE).

Ghalem BACHIR was born in Oran in Algeria. He is currently a professor at the University of Science and technology of Oran with a degree of professor of the universities. He is a team leader in the 'LDDEE' research laboratory whose main theme is research in renewable energies.

Michel AILLERIE obtained a PhD in 1991 and the Habilitation to Lead Researches in 2001 at the Université Paul Verlaine of Metz, currently Université de Lorraine. He is Professor since 2005 and makes his research in the city of Metz at the Laboratoire Materiaux Optiques et Photonique, LMOPS, join laboratory of the Université de Lorraine and CentraleSupelec – Université de Paris-Saclay, France. He is researcher in the team "Materials, Components and Systems for Photovoltaic" for which he is the leader. He collaborates in several national, European and international research projects and is co-general Chair of the TMREES International Conference series. He is author of more than 150 publications in international journals and in more than 250 international conference proceedings with selection on full text. He was regularly invited as speaker in international conferences and was guest editor of about 10 issues of international scientific revues. His interests and activities concern two main themes. The first one concerns the Characterization of functional non-linear optical properties of materials for optoelectronic applications. The second one concerns the development and optimization of energy production and management systems in a sustainable development approach.